

Supporting Information for

## Structure-Function Analysis of the Extended Conformation of a Polyketide Synthase Module

Xiuyuan Li<sup>†</sup>, Natalia Sevillano<sup>‡</sup>, Florencia La Greca<sup>‡</sup>, Lindsay Deis<sup>§</sup>, Yu-Chen Liu<sup>†</sup>, Marc C. Deller<sup>†,||</sup>, Irimpan I. Mathews<sup>||</sup>, Tsutomu Matsui<sup>||</sup>, David E. Cane<sup>∇</sup>, Charles S. Craik<sup>‡</sup>, Chaitan Khosla<sup>†,§,†,0\*</sup>

Departments of <sup>†</sup>Chemistry, <sup>§</sup>Biochemistry, and <sup>0</sup>Chemical Engineering, and <sup>†</sup>Stanford ChEM-H, Stanford University, Stanford CA 94305

<sup>‡</sup>Department of Pharmaceutical Chemistry, University of California San Francisco, San Francisco CA 94158

<sup>||</sup>Stanford Synchrotron Radiation Lightsource, SLAC National Accelerator Laboratory, Stanford University, Menlo Park CA 94025

<sup>∇</sup>Department of Chemistry, Box H, Brown University, Providence RI 02912-9108

\*Correspondence to: [khosla@stanford.edu](mailto:khosla@stanford.edu)

## Supplementary Figures

A

	CDR_L1	CDR_L2	CDR_L3
1B2	RSSQSLHSHNGYNYLD	LGSNRAS	MQSLQTPRLT
	CDR_H1	CDR_H2	CDR_H3
1B2	GFTFGDYAMS	GFIRSKAYGGTTE	TRGGTLFDY

B

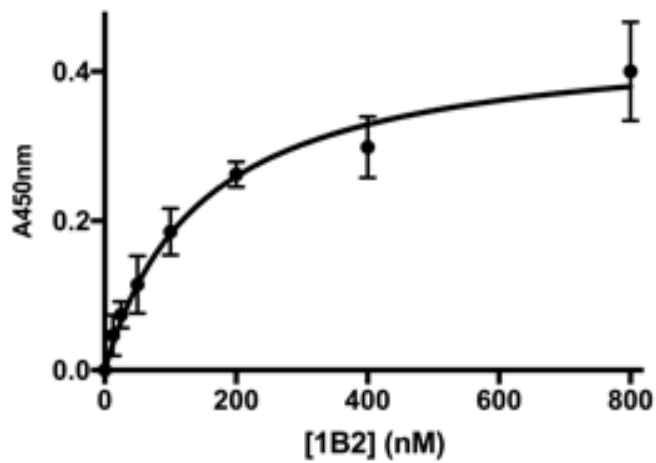


**Figure S1.** Properties of  $F_{ab}$  1B2: (A) Protein sequence of the complementarity determining regions (CDRs) of  $F_{ab}$  1B2. H: heavy chain; L: light chain. (B) Binding curve of 1B2 for the KS-AT fragment of Module 3+TE. Binding analysis was performed by ELISA.

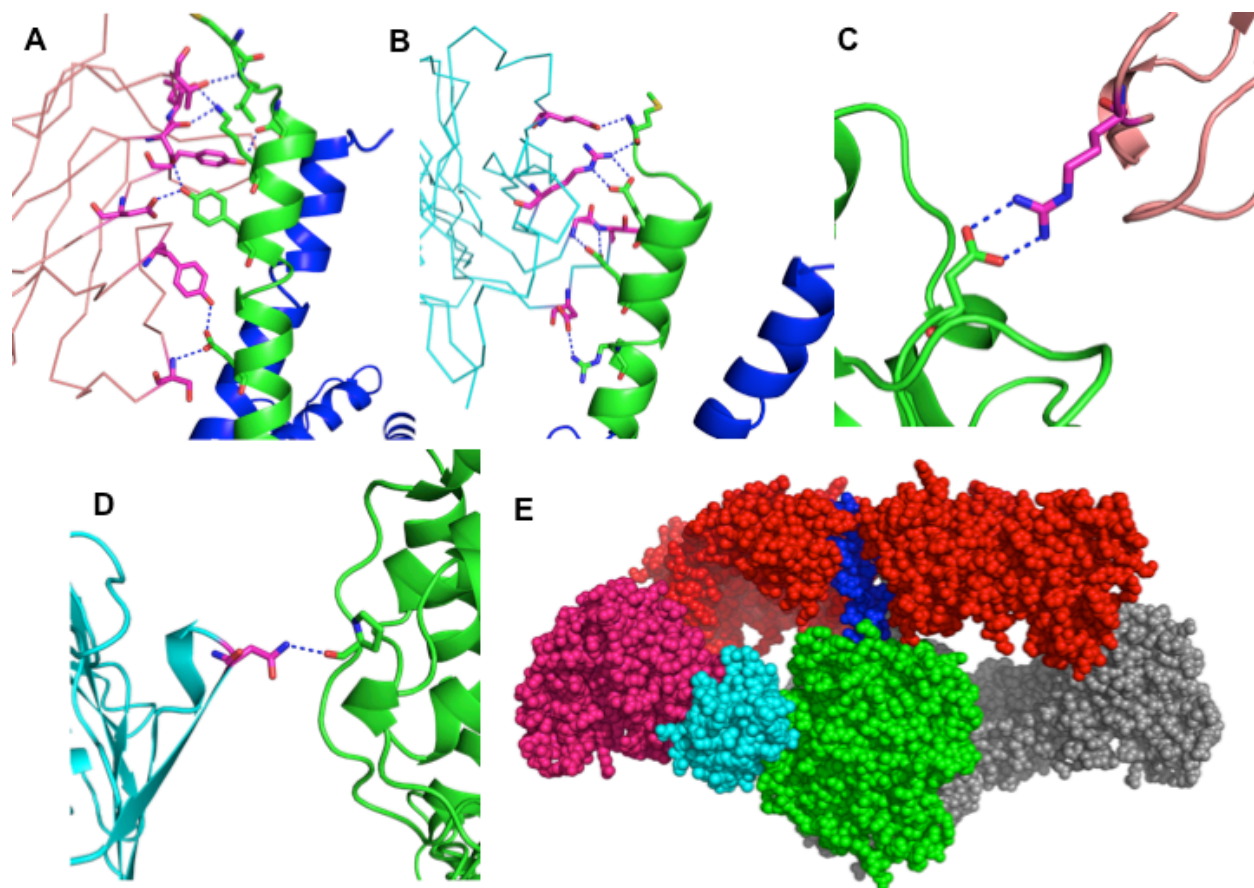


**Figure S2.** Detailed views of hydrogen bonds between 1B2 and one monomer of the homodimeric KS-AT fragment of DEBS Module 3: A full list of non-covalent interactions between 1B2 and this KS-AT monomer is provided in Table S1. KS-AT chains A and B are shown in green and blue, respectively, whereas the light and heavy chains of 1B2 are shown in pink and cyan, respectively. (A) H-bonding between the 1B2 light chains 1 and 2 and the docking domain in chain A of the KS-AT homodimer. (B) H-bonding between the 1B2 heavy chain 2 and the docking domain in chain A of the KS-AT homodimer. (C) H-bonding between Arp 98 on 1B2 light chain 1 and the Asp 331 on KS domain in chain A of the KS-AT homodimer. (D) H-bonding between Asn 211 on 1B2 heavy chain 2 and the Pro 775 on AT domain in chain A of the KS-AT homodimer. (E) Overall domain architecture of the 1B2/KS-AT complex. The calculated contact surface areas between antibody 1B2 and the docking domain, the KS domain, and the AT domain are 4397 Å<sup>2</sup>, 328 Å<sup>2</sup>, and 479 Å<sup>2</sup>, respectively.

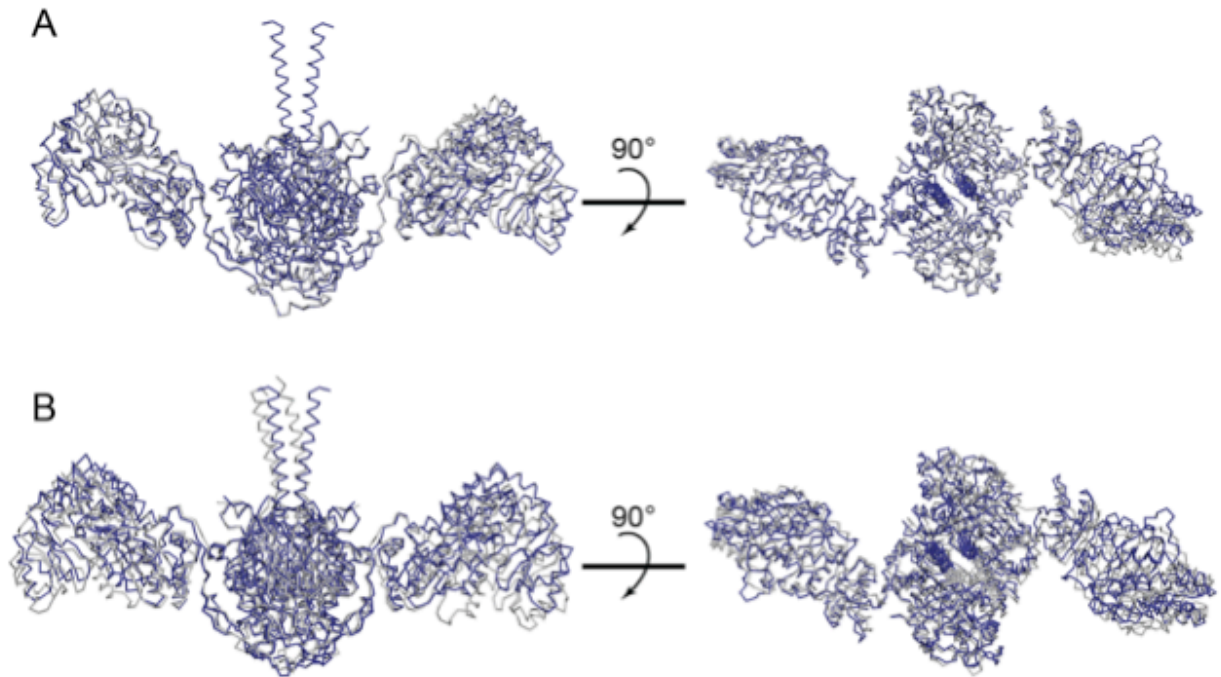


**Figure S3.** Backbone alignment of the homodimeric KS-AT fragment from the X-ray structure of the 1B2/KS-AT complex (blue) with X-ray structures of two free KS-AT dimers (gray): (A) Alignment (RMSD = 0.83 Å) with the KS-AT fragment from DEBS Module 3 lacking its docking domain (PDB 2QO3, ref 1). (B) Alignment (RMSD = 2.05Å) with the KS-AT fragment from DEBS Module 5 with its native N-terminal docking domain (PDB 2HG4, ref 2).

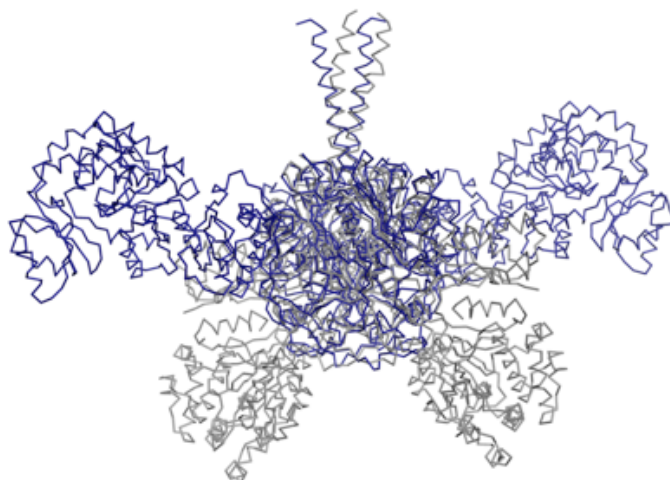


**Figure S4.** Backbone alignment of the homodimeric KS-AT fragment from the X-ray structure of the 1B2/KS-AT complex (blue) with the cryo-EM derived structure of the corresponding region of Module 5 of the pikromycin synthase (gray): While the docking domain and KS of the two complexes (residue 9-450) can be superimposed (local RMSD = 1.61Å), the respective KS-AT linker and AT regions display large scale differences in organization. The backbone atoms of 1B2 and the KR and ACP domains of Module 5 of the pikromycin synthase are hidden for clarity.

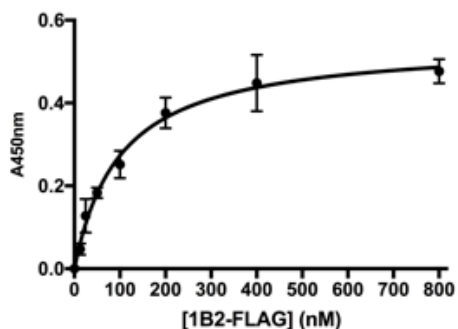


**Figure S5:** Binding analysis of 1B2 to DEBS Module 2+TE. Binding analysis was performed by ELISA. Each 1B2-FLAG concentration was analyzed in triplicate.

**Table S1.** X-ray data collection and refinement statistics for the 1B2/KS-AT complex\*

<b>Wavelength</b>	0.98
<b>Resolution range (Å)</b>	46.08 - 2.09 (2.17 - 2.09)
<b>Space group</b>	C2
<b>Cell dimensions</b>	
a, b, c (Å)	116.0, 140.0, 102.9
$\alpha$ , $\beta$ , $\gamma$ (°)	90.0, 97.1, 90.0
<b>Total reflections</b>	686056
<b>Unique reflections</b>	93105 (9210)
<b>Multiplicity</b>	7.4 (7.5)
<b>Completeness (%)</b>	98 (98)
<b>Mean I/sigma(I)</b>	19.8 (2.4)
<b>Wilson B-factor (Å<sup>2</sup>)</b>	28.8
<b>R-merge</b>	0.097 (0.744)
<b>R-meas</b>	0.104 (0.800)
<b>CC1/2</b>	0.999 (0.871)
<b>Reflections used in refinement</b>	89415 (8211)
<b>Reflections used for R-free</b>	1922 (182)
<b>R-work</b>	0.167 (0.196)
<b>R-free</b>	0.210 (0.235)
<b>Number of non-hydrogen atoms</b>	10561
macromolecules	9877
ligands	3
<b>Protein residues</b>	1311
<b>RMS (bonds) (Å)</b>	0.012
<b>RMS (angles) (°)</b>	1.38
<b>Ramachandran favored (%)</b>	95
<b>Ramachandran allowed (%)</b>	4.5
<b>Ramachandran outliers (%)</b>	0
<b>Rotamer outliers (%)</b>	0.39
<b>Clashscore</b>	3.01
<b>Average B-factor</b>	45.82
macromolecules	46.06
ligands	37.67
solvent	42.34

\*Statistics for the highest-resolution shell are shown in parentheses.

**Table S2.** SAXS data collection and analysis of 1B2 complexed with Module 2 in States A, B, and D (see Fig. 3 for state definitions).

	<b>State A</b>	<b>State B</b>	<b>State D</b>
<b>Data collection parameters</b>			
Instrument	SSRL BL4-2	SSRL BL4-2	SSRL BL4-2

Type of Experiment	SEC-SAXS	SEC-SAXS	Equilibrium SAXS
Defining slits size (H mm × V mm)	0.25× 0.25	0.25× 0.25	0.25× 0.25
Detector distance (m)	2.5	2.5	2.5
Detector	Rayonix MX225-HE	Pilatus3 X 1M	Pilatus3 X 1M
Beam energy (keV)	12.4	12.4	12.4
$q$ range ( $\text{\AA}^{-1}$ )	0.049–0.36	0.052–0.34	0.0077–0.40
Exposure time/frame (s)	1	1	1
Frames per data set	700	700	10
Temperature (K)	293	293	293
<b>SEC parameters</b>			
SEC column	Superose 6 Increase PC 3.2/300	Superose 6 Increase PC 3.2/300	Superose 6 Increase PC 3.2/300
Amount loaded (nmol)	0.64-1.92	0.48-2.86	0.49 - 1.22
HPLC flow rate (mL/min)	0.04	0.04	0.04
<b>Structural parameters</b>			
$I(0)$ from Guinier	$1664.95 \pm 5.16$	$32.83 \pm 0.18$	$17.30 \pm 0.06$
$R_g$ ( $\text{\AA}$ ) from Guinier	$66.51 \pm 3.07$	$66.18 \pm 4.37$	$63.79 \pm 4.64$
$I(0)$ from $P(r)$	1602	31.47	17
$R_g$ ( $\text{\AA}$ ) from $P(r)$	63.97	63.55	63.07
$D_{\max}$ ( $\text{\AA}$ ) from $P(r)$	200	199	200
Porod volume estimate ( $\text{\AA}^3$ )	1090000	1150000	1150000
<b>Software employed</b>			
Primary data reduction	SasTool	SasTool	SasTool
Data processing	PRIMUS	PRIMUS	PRIMUS
		<b>Extended conformation</b>	<b>Arched conformation</b>
<b>Curve fitting using atomic model</b>			
Software employed		CRYSOL	CRYSOL
Predicted $R_g$ ( $\text{\AA}$ )		60.54	63.88
Predicted $D_{\max}$ ( $\text{\AA}$ )		187.4	212.8
$q$ range ( $\text{\AA}^{-1}$ )		0.094-0.20	0.094-0.20



**Table S3.** *Non-covalent contacts ( $\leq 3.6\text{\AA}$ ) at the 1B2/KS-AT interface.* All hydrogen bonds (bold) and van der Waals contacts between one KS-AT monomer (chain A) and antibody 1B2 (Chain L = light chain 1, chain M = light chain 2, chain H = heavy chain 1, chain N = heavy chain 2) are listed. Heavy chain 1 does not contact chain A. Hydrogen bonds are shown explicitly in Figure S2.

Residues from KS/AT			Residues from 1B2 (light chain 1)			Distance
Ser	5A	CB	Ser	48L	CB	3.60
Ser	5A	CB	Ser	48L	C	3.62
Ser	5A	CB	Asn	49L	N	3.58
Ser	5A	OG	Ser	48L	CB	3.55
Ser	5A	OG	His	47L	CE1	3.38
Ser	5A	O	Asn	49L	CA	3.64
Ala	9A	CA	Asn	49L	O	3.53
Ala	9A	CB	Asn	49L	O	3.17
Leu	12A	CG	Tyr	51L	OH	3.63
Leu	12A	CD2	Tyr	51L	CE1	3.53
Arg	23A	CZ	Arg	75L	O	3.43
Arg	23A	NH1	Arg	75L	O	3.23
Arg	23A	NH2	Ser	77L	N	3.39
Arg	23A	NH2	Ser	77L	CA	3.64
<b>Arg</b>	<b>23A</b>	<b>NH2</b>	<b>Arg</b>	<b>75L</b>	<b>O</b>	<b>2.79</b>
Asp	331A	CG	Arg	98L	NH1	3.25
Asp	331A	CG	Arg	98L	NH2	3.58
Asp	331A	OD1	Arg	98L	CZ	3.19
Asp	331A	OD1	Arg	98L	NH1	2.99
<b>Asp</b>	<b>331A</b>	<b>OD1</b>	<b>Arg</b>	<b>98L</b>	<b>NH2</b>	<b>2.76</b>
<b>Asp</b>	<b>331A</b>	<b>OD2</b>	<b>Arg</b>	<b>98L</b>	<b>NH1</b>	<b>2.82</b>

Residues from KS/AT			Residues from 1B2 (light chain 2)			Distance
Met	1A	CB	Thr	115M	O	3.17
Met	1A	CG	Thr	115M	O	2.87
Met	1A	SD	Thr	115M	O	2.78
<b>Val</b>	<b>2A</b>	<b>N</b>	<b>Thr</b>	<b>115M</b>	<b>OG1</b>	<b>3.01</b>
Val	2A	CB	Thr	115M	OG1	3.50
Val	2A	O	Thr	115M	OG1	3.64
Asp	4A	CG	His	47M	NE2	3.44
<b>Asp</b>	<b>4A</b>	<b>OD1</b>	<b>Tyr</b>	<b>53M</b>	<b>OH</b>	<b>3.22</b>
Asp	4A	OD1	His	47M	NE2	3.33
Asp	4A	OD1	His	47M	CD2	3.65
Asp	4A	OD2	His	47M	NE2	3.48
Lys	7A	CD	Ser	112M	O	3.29
Lys	7A	CE	Ser	112M	O	3.48

<b>Lys</b>	<b>7A</b>	<b>NZ</b>	<b>Ser</b>	<b>112M</b>	<b>O</b>	<b>2.83</b>
Lys	7A	NZ	Leu	113M	C	3.39
<b>Lys</b>	<b>7A</b>	<b>NZ</b>	<b>Leu</b>	<b>113M</b>	<b>O</b>	<b>2.79</b>
Val	8A	CG2	Tyr	53M	OH	3.52
Tyr	11A	CD1	Leu	71M	CG	3.65
Tyr	11A	CE1	Asp	55M	OD1	3.59
Tyr	11A	CZ	Asp	55M	OD2	3.58
Tyr	11A	OH	Asp	55M	CG	3.38
Tyr	11A	OH	Asp	55M	OD1	3.44
<b>Tyr</b>	<b>11A</b>	<b>OH</b>	<b>Asp</b>	<b>55M</b>	<b>OD2</b>	<b>2.57</b>
Tyr	11A	OH	Ser	112M	CB	3.24
<b>Tyr</b>	<b>11A</b>	<b>OH</b>	<b>Ser</b>	<b>112M</b>	<b>OG</b>	<b>2.90</b>
Arg	14A	CG	Tyr	70M	CE1	3.57
Arg	14A	CG	Tyr	70M	CZ	3.61
Ala	15A	N	Tyr	70M	OH	3.58
Ala	15A	CA	Tyr	70M	OH	3.46
Asp	18A	CG	Ser	77M	N	3.56
<b>Asp</b>	<b>18A</b>	<b>OD1</b>	<b>Ser</b>	<b>77M</b>	<b>N</b>	<b>2.91</b>
Asp	18A	OD1	Ser	77M	CA	3.63
Asp	18A	OD1	Ser	77M	CB	3.14
Asp	18A	OD2	Tyr	70M	CE1	3.59
Asp	18A	OD2	Tyr	70M	CZ	3.60
<b>Asp</b>	<b>18A</b>	<b>OD2</b>	<b>Tyr</b>	<b>70M</b>	<b>OH</b>	<b>2.74</b>

Residues from KS/AT			Residues from 1B2 (heavy chain 2)			Distance
<b>Met</b>	<b>1A</b>	<b>O</b>	<b>Arg</b>	<b>54N</b>	<b>NH2</b>	<b>3.06</b>
Met	1A	N	Glu	63N	OE1	3.43
Met	1A	N	Glu	63N	CD	3.46
<b>Met</b>	<b>1A</b>	<b>N</b>	<b>Glu</b>	<b>63N</b>	<b>OE2</b>	<b>2.92</b>
Met	1A	CA	Glu	63N	OE1	3.63
Met	1A	CA	Glu	63N	OE2	3.60
Glu	6A	CG	Tyr	58N	CD1	3.50
Glu	6A	CD	Arg	54N	NE	3.51
Glu	6A	CD	Arg	54N	NH2	3.59
<b>Glu</b>	<b>6A</b>	<b>OE1</b>	<b>Arg</b>	<b>54N</b>	<b>NH2</b>	<b>2.94</b>
Glu	6A	OE2	Arg	54N	CD	3.47
<b>Glu</b>	<b>6A</b>	<b>OE2</b>	<b>Arg</b>	<b>54N</b>	<b>NE</b>	<b>2.64</b>
Glu	6A	OE2	Arg	54N	CZ	3.51
Glu	6A	OE2	Arg	54N	NH2	3.49
Glu	6A	OE2	Tyr	58N	CB	3.57
Glu	6A	OE2	Tyr	58N	CD1	3.65
Lys	7A	CG	Thr	105N	OG1	3.51
Ala	9A	CB	Tyr	58N	OH	3.40
Glu	10A	CD	Gly	104N	N	3.36

Glu	10A	CD	Thr	105N	N	3.59
Glu	10A	OE1	Gly	104N	N	3.27
<b>Glu</b>	<b>10A</b>	<b>OE1</b>	<b>Thr</b>	<b>105N</b>	<b>N</b>	<b>2.86</b>
Glu	10A	OE1	Thr	105N	CA	3.47
Glu	10A	OE1	Thr	105N	CB	3.52
Glu	10A	OE1	Thr	105N	C	3.60
Glu	10A	OE1	Leu	106N	N	2.81
Glu	10A	OE2	Gly	103N	CA	3.62
Glu	10A	OE2	Gly	103N	C	3.62
<b>Glu</b>	<b>10A</b>	<b>OE2</b>	<b>Gly</b>	<b>104N</b>	<b>N</b>	<b>2.70</b>
Glu	10A	OE2	Gly	104N	CA	3.55
Arg	13A	CD	Tyr	34N	CZ	3.26
Arg	13A	CD	Tyr	34N	OH	3.12
Arg	13A	CD	Tyr	34N	CE2	3.45
Arg	13A	NH1	Tyr	34N	CE2	3.43
Arg	13A	NH1	Tyr	34N	CD2	3.37
Arg	13A	NH2	Asp	33N	O	3.49
Arg	13A	CD	Tyr	34N	CZ	3.56
Arg	13A	CD	Tyr	34N	OH	3.41
Arg	14A	CD	Asp	108N	OD2	3.54
Arg	14A	NH1	Arg	102N	NH2	3.57
<b>Arg</b>	<b>14A</b>	<b>NH1</b>	<b>Asp</b>	<b>108N</b>	<b>OD2</b>	<b>2.83</b>
Leu	17A	CD1	Tyr	34N	OH	3.04
<b>Pro</b>	<b>775A</b>	<b>O</b>	<b>Asn</b>	<b>211N</b>	<b>ND2</b>	<b>2.91</b>
Pro	777A	CD	Asn	211N	OD1	3.40

## Experimental Methods

**Cloning, expression, and purification of DEBS proteins:** DEBS proteins were expressed in *E. coli*, and purified according to protocols previously described<sup>3-6</sup>. Briefly, *E. coli* BAP1 cells<sup>7</sup> containing the appropriate plasmid were cultured in LB media, supplemented with carbenicillin (100 µg/mL) or kanamycin (50 µg/mL). Cultures (1 L) were inoculated with overnight seed culture at v/v=200:1, shaken at 37 °C and 220 rpm until an OD<sub>600</sub> of 0.5-0.8 was attained, then cooled to 18 °C, and induced with 250 µM isopropyl-β-D-thiogalactopyranoside (IPTG). Cells were harvested after 12-16 h by centrifugation at 6,300 g for 5 min, and resuspended in lysis buffer (50 mM phosphate, pH 7.6, 10 mM imidazole, 450 mM NaCl, 20% (v/v) glycerol) supplemented with a protease inhibitor cocktail (Complete<sup>TM</sup>, Roche). Cells were then lysed by sonication, and the lysate was clarified by centrifugation (30,000 g, 120 min). The supernatant was incubated with 4 mL of Ni-NTA resin (Invitrogen, 50% slurry, pre-equilibrated with lysis buffer) for 1 h at 4 °C. The resin was washed with (i) five column volumes (CV) of lysis buffer; (ii) 5 CV of 50 mM phosphate, pH 7.6, 50 mM imidazole, 300 mM NaCl, 10 % glycerol (v/v); (iii) 3 CV of 50 mM phosphate, pH 7.6, 500 mM imidazole, 40 mM NaCl, 10 % glycerol (v/v). The eluant was applied to a 5 mL HiTrapQ HP column (GE Healthcare) and washed with 5 CV of FPLC Buffer A (50 mM phosphate, pH 7.6, 10% (v/v) glycerol). Proteins were eluted with a gradient 0-100% FPLC Buffer B (50 mM phosphate, pH 7.6, 500 mM NaCl, 10% (v/v) glycerol) over 40 CV. The eluted fractions were pooled and concentrated in a Centricon filter (Millipore) with an appropriate molecular weight cut-off. Final protein concentrations were quantified with BCA assay (Pierce).

**F<sub>ab</sub> selection and verification:** A fully human naïve F<sub>ab</sub> phage display library<sup>8</sup> was used to identify specific antibody fragments against target antigens. The panning was performed according to protocols described previously<sup>9</sup> with DEBS Module 3+TE, lightly biotinylated with NHS-PEG<sub>12</sub>-biotin reagent (EZ-Link<sup>TM</sup>), immobilized on streptavidin-coated magnetic beads. After three rounds of panning, small scale F<sub>ab</sub> cultures were prepared from individual clones in a 96-well format. Culture supernatants were screened for binding to Module 3+TE by ELISA. Clones with a positive signal in ELISA were sequenced and used for further analysis.

**ELISA measurement of binding affinity:** ELISA assays were performed as previously reported<sup>10</sup>. In brief, wells of Maxisorp plates (Nunc) were coated with 50 µL of streptavidin (Promega, 5 µg/mL in PBS) overnight at 4 °C. Wells were washed twice with PBS and blocked by shaking with 300 µL of PBS containing 5 % (w/v) bovine serum albumin (BSA) for 1 h at room temperature. Wells were washed 3 times with protein buffer (400 mM phosphate pH 7.2). The biotinylated target protein (50 µL of 10–20 µg/mL in protein buffer containing 2 % BSA) or protein buffer alone was added to each well. Plates were shaken at room temperature for 30 min followed by three washes with protein buffer. Purified F<sub>ab</sub> or F<sub>ab</sub>-containing culture media in 2 % BSA/protein buffer was added to each well for 1 h. Wells were washed 3 times with protein buffer containing 0.05% Tween-20, followed by the addition of 50 µL of 0.3 µg/mL anti-Myc or anti-FLAG antibody conjugated to peroxidase (ThermoFisher) in protein buffer containing 2% BSA. Plates were shaken at room temperature for 1 h, followed by 3 washes with 0.05% (v/v) Tween-20 in protein buffer and finally one wash with protein buffer alone. 50 µL of Turbo TMB (Pierce) was added to each well. Plates were incubated without shaking until the blue color

appeared. Reactions were stopped with 20  $\mu$ L 2.5M H<sub>2</sub>SO<sub>4</sub>, and absorbance was read at 450 nm.

**Expression and periplasmic extraction of F<sub>ab</sub>:** *E. coli* BL21(DE3) cells harboring the F<sub>ab</sub> encoding plasmid were grown in 2xYT or Terrific Broth medium with carbenicillin (100  $\mu$ g/mL) and 0.1 % (w/v) glucose at 37 °C and 250 rpm until an O.D.<sub>600</sub> of 0.6-0.8 was attained. The cultures were then cooled to 20 °C, induced with the addition of 1 mM IPTG, and allowed to grow for 12-14 h at 180 rpm. The bacteria were pelleted by centrifugation at 6,300 g for 10 min. The cells were re-suspended by gently stirring in 20 mL of TES buffer (0.2 M Tris, pH 8.0, 0.5 mM ethylenediaminetetraacetic acid (EDTA), 0.5 M sucrose) for 2 h at 4 °C. Then 20 mL of deionized water containing protease inhibitor cocktail (Roche) was added. The solution was further stirred at 4 °C for 2 h, and cells were pelleted at 25,000 g. The supernatant was supplemented with 2 mM MgCl<sub>2</sub> and 10mM imidazole, and incubated overnight with 2 mL Ni-NTA agarose pre-equilibrated with wash buffer I (250 mM NaCl, 50 mM Tris, pH 8.0). The Ni-NTA resin was then washed with 5 CV of wash buffer I followed by 5 CV of wash buffer II (20 mM imidazole, 500 mM NaCl, 50 mM Tris, pH 8.0), and the F<sub>ab</sub> was eluted with 3 CV of the elution buffer (500 mM imidazole, 100 mM NaCl, 50 mM Tris, pH 8.0). The eluted fractions were concentrated to 500  $\mu$ L for size-exclusion chromatography on Superdex 200 10/30 (GE Healthcare) in 10 mM HEPES, 250 mM NaCl, pH 8.0 (SEC buffer). The F<sub>ab</sub> concentration was quantified by BCA assay (Pierce).

#### **Enzymatic assays with Module 2+TE:**

Kinetic assays to probe intermodular chain translocation and intramodular chain elongation have been developed and extensively utilized in previous work from our laboratories<sup>4, 11-15</sup>. By definition, at low [acyl-ACP] values, the slopes of the curves in the left graph of Fig. 6 reflect conditions where intermodular chain translocation is the limiting step for turnover, whereas turnover is limited by intramodular chain elongation under saturating conditions. For pragmatic reasons, it is not always possible to achieve full saturation in  $v$  versus [S] measurements involving ACP substrates. To be sure that observed differences under near-saturation conditions are not meaningful, we conducted an additional experiment using an SNAC ester substrate, which can be readily used at concentrations exceeding 10 mM, where full saturation is achieved.

Briefly, 2  $\mu$ M DEBS Module 2+TE and F<sub>ab</sub> at variable concentrations were added into 400 mM sodium phosphate, pH 7.2, containing 5 mM TCEP, 10 mM MgCl<sub>2</sub>, 2 mM Coenzyme A, and 2.5 mM ATP. Enzymes MatB (2  $\mu$ M) and methylmalonyl-CoA epimerase (4  $\mu$ M) were included to convert methylmalonic acid into racemic methylmalonyl-CoA<sup>16</sup>. Chain elongation kinetic analysis was initiated upon simultaneous addition of (2S,3R)-2-methyl-3-hydroxypentanoyl-N-acetylcysteamine thioester (NDK-SNAC) at variable concentrations<sup>17</sup>, 1 mM methylmalonic acid, and 1 mM NADPH<sup>6</sup>. Chain translocation assays were performed with NDK-ACP1 at variable concentrations<sup>18</sup>, 1 mM methylmalonic acid, and 1 mM NADPH<sup>5</sup>. Reaction progress was followed by monitoring depletion of NADPH in an Eppendorf cuvette at 340 nm using a Lambda-25 UV-Vis Spectrophotometer (Perkin-Elmer).

**Crystallization:** The F<sub>ab</sub>/KS-AT complex was produced by incubating the antigen with a slight molar excess of F<sub>ab</sub> for at least 30 min at 4 °C, followed by SEC purification using Superdex 200 10/300 SEC (GE Healthcare) pre-equilibrated with SEC buffer. Fractions corresponding to the complex were pooled and concentrated. Crystals of form 1 (space group C2) were obtained by combining 0.5 μL of protein at 9.1 mg/mL in SEC buffer with 0.5 μL of screen (200 mM potassium citrate, 20%(w/v) PEG 3,350 and 12%(v/v) ethylene glycol) at 12°C. Crystals of form 2 (space group P<sub>21</sub>) were obtained by combining 0.15 μL of protein at 9.5 mg/mL in SEC buffer with 0.15 μL of screen (200 mM di-ammonium tartrate, 20%(w/v) PEG 3,350 and 15%(v/v) ethylene glycol) at 12°C. Crystals were grown for 6 weeks and harvested by direct immersion in liquid N<sub>2</sub> without extra cryoprotectant. Data were collected on BL 11-1 and 12-2 at the Stanford Synchrotron Radiation Lightsource at 100 K, and processed with HKL2000<sup>19</sup>.

The structure was determined using molecular replacement as implemented by PHASER<sup>20</sup> using the KS-AT fragment of Module 3 (PDB code 2QO3) and an F<sub>ab</sub> analog (PDB code 1SBS). The initial model was built in PHENIX AutoBuild<sup>21</sup> and subsequent model building was performed using COOT<sup>22</sup>. Refinement was performed using *phenix.refine*<sup>23</sup> with isotropic B factors for all atoms. Alternative conformations were modeled using COOT<sup>22</sup>. The final refined model converged with R<sub>work</sub> and R<sub>free</sub> values of 16.7% and 21.0%, respectively. Coordinates were analyzed for all-atom contacts and correct geometry using MolProbity<sup>24</sup>, and the final coordinates were deposited in the Protein Data Bank as PDB ID 6C9U.

**Tandem size exclusion chromatography and small angle X-ray scattering (SEC-SAXS):** SEC-SAXS analysis was performed on the Bio-SAXS beam line BL 4-2 at Stanford Synchrotron Radiation Lightsource (SSRL) following previous protocol with slight modification<sup>3</sup>. A Pilatus 1M detector was used with a sample-to-detector distance of 2.5 m and a beam energy of 12.4 keV ( $\lambda = 0.9998 \text{ \AA}$ ). The momentum transfer (scattering vector)  $q$  was defined as  $q = 4\pi\sin(\theta)/\lambda$ , where  $2\theta$  is the scattering angle. The  $q$  scale was calibrated by silver behenate powder diffraction. All data were collected up to a maximum  $q$  of  $0.40 \text{ \AA}^{-1}$  (2.5 m sample-to-detector distance).

For the 1B2/Module 2 complex in state A (**Fig. 3**), the antibody and PKS homodimer was mixed at room temperature for 60 min in a 1.2:1 stoichiometry, then chromatographed at 0.04 mL/min on a Superose 6 Increase 3.2/300 column (GE Healthcare) equilibrated with 200 mM Na-phosphate, pH 7.6. Importantly, all SEC-SAXS experiments were performed in the buffer defined above, because maximum PKS activity critically depends on the presence of high phosphate concentrations. In-line SAXS analysis was performed as the eluted complex passed into the detection capillary.

Whereas State A corresponds to the unoccupied *holo*-protein, State B corresponds to the module with its KS active site covalently bound to the diketide substrate. This state is stable for over 60 min after desalting, considerably longer than the time required for SEC-SAXS analysis (~40 min). State D corresponds to the module with an elongated triketide product bound to its ACP domain. We have shown that 1 min incubation is sufficient for enzyme to complete elongation, and the hallmark “turnstile” associated with this state of the module has a lifetime of

~15 min<sup>11</sup>. These samples were subjected immediately to SEC-SAXS analysis. To prepare Module 2 in state B (**Fig. 3**), the complex was pre-treated with 5mM NDK-SNAc<sup>17</sup> (~100 equiv) for 10 min at room temperature before injection onto the SEC column. To prepare Module 2 in state D (**Fig. 3**), fresh state B peak fractions were rapidly mixed with 2.5 mM methylmalonyl-CoA and 0.5 mM NADPH for 1 min to initiate chain elongation reaction. The resulting mix was then injected into the capillary for equilibrium SAXS analysis. A sample of State B without the chain elongation mix was also included as a control.

In order to evaluate the validity of SAXS-derived solution structural models, we built rigid body F<sub>ab</sub> docking models in both extended and arched conformations to generate theoretical SAXS scattering curves. Since the KS domains from the 1B2-KS/AT crystal structure, SAXS and EM models showed minimal structural deviation, we aligned the KS portion of the crystal structures from the 1B2-KS/AT crystal structure to KS of the extended and arched conformations (Fig. 7A). In each case, the 1B2 does not clash with the PKS protein. The resulting structures were input into CRYSOLO to generate the simulated curves (blue and red curves in Fig. 7B&C) and subsequently compared with scattering data (black curves in Fig. 7B&C).

Since marginal concentration-dependent inter-particle interactions were observed on state B (SEC-SAXS) and state D data (Equilibrium SAXS), final curves used for curve fitting were generated by merging curves at different injection volume and concentration data, respectively. The details of SAXS data collection and analysis are listed in Table 2.

**Illustrations:** All structural illustrations were made in PyMOL (Schrödinger, LLC)

**Accession codes:** Molecular coordinates and structure factors have been deposited in Protein Data Bank with accession code 6C9U.

## References

1. Tang, Y.; Chen, A.Y.; Kim, C.Y.; Cane, D.E.; Khosla, C. *Chem. Biol.* **2007**, 14, 931.
2. Tang, Y.; Kim, C.Y.; Mathews, I.I.; Cane, D.E.; Khosla, C. *Proc. Natl. Acad. Sci.* **2006**, 103, 11124.
3. Edwards, A.L.; Matsui, T.; Weiss, T.M.; Khosla, C. *J. Mol. Biol.* **2014**, 426, 2229.
4. Lowry, B.; Robbins, T.; Weng, C.H.; O'Brien, R.V.; Cane, D.E.; Khosla, C. *J. Am. Chem. Soc.* **2013**, 135, 16809.
5. Wu, N.; Cane, D.E.; Khosla, C. *Biochemistry* **2002**, 41, 5056.
6. Chen, A.Y.; Schnarr, N.A.; Kim, C.Y.; Cane, D.E.; Khosla, C. *J. Am. Chem. Soc.* **2006**, 128, 3067.
7. Pfeifer, B.A.; Admiraal, S.J.; Gramajo, H.; Cane, D.E.; Khosla, C. *Science* **2001**, 291, 1790.
8. Duriseti, S.; Goetz, D.H.; Hostetter D.R.; LeBeau, A.M.; Wei, Y.; Craik, C.S. *J. Biol. Chem.* **2010**, 285, 26878.
9. Kim, J.; Stroud, R.M.; Craik, C.S. *Methods* **2011**, 55, 303.
10. Kim, J.; Wu, S.; Tomasiak, T.M.; Mergel, C.; Winter, M.B.; Stiller, S.B.; Robles-Colmaneraers, Y.; Stroud, R.M.; Tampe, R.; Craik, C.S.; Cheng, Y. *Nature* **2014**, 517, 396.
11. Lowry, B.; Li, X.; Robbins, T.; Cane, D.E.; Khosla, C. *ACS Cent Sci* **2016**, 2, 14.
12. Wu, N.; Kudo, F.; Cane, D.E.; Khosla, C. *J. Am. Chem. Soc.* **2000**, 122, 4847

13. Wu, N.; Tsuji, S.; Cane, D.E.; Khosla, C. *J. Am. Chem. Soc.* **2001**, 123, 6465
14. Wu, N.; Cane, D.E.; Khosla, C. *Biochemistry*, **2002**, 41, 5056
15. Wu, J.; Kinoshita, K.; Khosla, C.; Cane, D.E. *Biochemistry*, **2004**, 42, 16301
16. Hughes, A.J.; Keatinge-Clay, A.T. *Chem. Biol.* **2011**, 18, 165.
17. Jacobsen, J.R.; Hutchinson, C.R.; Cane, D.E.; Khosla, C. *Science* **1997**, 277, 367.
18. Ostrowski, M.P.; Cane, D.E.; Khosla, C. *J. Antibiot.* **2016**, 69, 507.
19. Otwinowski, Z.; Minor, W. *Methods Enzymol.* **1997**, 276, 307.
20. McCoy, A.J.; Grosse-Kunstleve, R.W.; Adams, P.D.; Winn, M.D.; Storoni, L.C.; Read, R.J. *J. Appl. Cryst.* **2007**, 40, 658.
21. Terwilliger, T.C.; Grosse-Kunstleve, R.W.; Afonine P.V.; Moriarty, N.W.; Zwart, P.H.; Hung, L.W.; Read, R.J.; Adams, P.D. *Acta Crystallogr D Biol Crystallogr* **2007**, 64, 61.
22. Emsley, P.; Lohkamp, B.; Scott, W.; Cowtan, K. *Acta. Crystallogr. D Biol. Cryst.* **2010**, 66, 486.
23. Adams, P.D.; Afonine P.V.; Bunkoczi, G.; Chen, V.B.; Davis, I.W.; Echols, N.; Headd J.J.; Hung, L.W.; Kapral, G.J.; Grosse-Kunstleve, R.W.; McCoy, A.J.; Moriarty, N.W.; Oeffner, R.; Read, R.J.; Richardson, D.C.; Richardson, J.S.; Terwilliger, T.C.; Zwart, P.H. *Acta. Crystallogr. D Biol. Cryst.* **2010**, 66, 213.
24. Chen, V.B.; Arendall, W.B.; Headd, J.J.; Keedy, D.A.; Immormino, R.M.; Kapral, G.J.; Murray, L.W.; Richardson, J.S.; Richardson, D.C. *Acta. Crystallogr. D Biol. Cryst.* **2010**, 66, 12.